Extended Kalman Filter Based Modelled Predictor for Fusion of Accelerometer and Camera Signal to Estimate the Vibration of a Mobile Flexible Link Manipulator

Tai Kiang Chang, Jee-Hou Ho
Department of Mechanical, Materials and Manufacturing Engineering, Faculty of Engineering, The University of Nottingham, Malaysia Campus, Selangor Darul Ehsan, Malaysia
keyx7tc@nottingham.edu.my

***Abstract*---This paper presents the fusion of accelerometer and camera for active vibration prediction for a mobile flexible link manipulator based on Extended Kalman filter-based modelled predictor. The tip position of the manipulator is unpredictable due to the singularity of the mobile flexible manipulator, as well as the phase lag in the control system due to the time delay between the sensor feedback and the control input. The purpose is thus to improve the prediction accuracy of the tip position. The time delayed in camera data estimates is used to correct the drifting accelerometer's signal. The dynamic model of the mobile flexible link manipulator is derived and is used to feed to the prediction stage of the Extended Kalman filter, which is used for vibration prediction. In order to investigate the efficiency of the proposed method, simulation and experimental studies are performed considering a single link flexible manipulator on a wheeled base. Experimental verifications showed that the proposed method produced good vibration prediction of the mobile manipulator compared to other model based predictor.**

***Index terms*---Mobile Flexible Manipulator; Sensor Fusion; Extended Kalman Filter; Model Based Prediction.**

I. INTRODUCTION

Mobile flexible link manipulators (MFLM) are going beyond industrial and space robotic applications due to their wide area of the workspace, smaller footprint, smaller actuators, better maneuverability and faster as compared to their fixed rigid counterpart [1, 2]. The key objective for the use of flexible link manipulators is to reduce the power consumption, increase payload-to-weight ratio, increase the speed of performances, and reduce the overall weight of the robot. However, due to the nonlinearity and non-minimum phase characteristics of the flexible manipulator, as well as the non-collocation of sensors, feedback lag in the estimation errors are inevitable [3].

To improve the measurement accuracy and provide real-time feedback for the control system, Kalman filter [4] is frequently used to fuse the measurements from both strain gauges (or accelerometer) and camera. Luca and Paolo [4] fused strain gauge and camera with LED at the tip of the flexible manipulator using Kalman filter for tip vibration sensing. Dubus [5] proposed an online delay estimator based on a cross-correlation technique that computes the time-delay between the camera and accelerometer.

A predictive sensor system would provide accurate sensor feedback and prediction to the control on flexible manipulator on a mobile base and thus an area to explore owing to complex and strongly coupled dynamics of the mobile platform and the singularity of the flexible arm. Having a feedback system to predict and track the flexible beam vibration, the predictive control can regulate control input to attain desired end-effector trajectory and vibration minimisations rather than using a point-to-point manoeuvre.

The study of vibration estimation and prediction of a flexible beam could also be extended to other applications, for example, for developing advanced feedback to controllers for flexible structures. In order to perform a task which requires high precision, it is crucial to acquire the actual position of the tip of the flexible manipulator. With the information of the tip vibration, the controller would be able to control the actuator at the hub accurately so as to reduce the vibration and improve the positioning at the tip. Consider an application of a mobile robot painting the wall; the controller would require the position of the brush and also the magnitude of the vibration at the tip in order to produce a smooth painting. Accurate prediction of the tip position of the MFLM will greatly improve motion planning of the mobile base. Thus, this study provides beneficial explorations into accurate motion planning of the mobile platform with the flexible manipulator.

The controllers for the flexible manipulators have been extensively studied for more than two decades [2]. Researchers who addressed this issue from a predictive control point of view mainly followed either classical predictive approaches or modern predictive approaches, which are mainly model-based [6]. Common classical predictive approaches include Smith predictor and internal model control (IMC). Modern predictive approaches include model-based predictive controls (MPC) [7], such as the generalized predictive control (GPC). The success of these predictive control methods is their ability to explicitly handle constraints, nonlinear systems [8], and processes with feedback delay or lag [3].

In model-based control, closed-loop stability is assured assuming that the truncated vibration modes do not affect the robot's dynamics [9]. This approach only considers present states in states prediction. To improve the accuracy of the prediction, Ghahramani, and Towhidkhah [10]

proposed a new incremental form of the GPC algorithm with input constraint, where both present and previous states were considered. However, the model-based control may lead to unsatisfactory performance when an accurate model is unavailable, due to parameters uncertainty or truncation of high order vibration modes. It is difficult to model such system due to its unknown vibrational behaviour. Furthermore, model-based control does not provide robustness to external disturbances [9]. The study for a predictive controller for active vibration suppression is thus still lacking [8], making it an exploitable research area.

This work focuses on the development of a low cost predictive sensor system to estimate the vibration of a flexible manipulator. Fusion of accelerometer and camera using Extended Kalman filter based model predictor is used to estimate the vibration at the tip of flexible beam.

The organization of this article is as follows. Section 2 is the problem formulation. Section 3 derives the model of MFLM. Section 4 describes the sensor system used in this work. Section 5 outlines the proposed Extended Kalman filter (EKF) algorithm. The experimental results and performance comparison of different types of EKF algorithms are included in Section 6. Finally, the conclusion is presented in Section 7.

II. Problem Formulation

The sensor system used in this work consists of accelerometer and camera. The accelerometer provides an instant feedback to the motion of the beam tip with cumulative position errors. This is caused by high random noise and time-varying bias possess in accelerometer. The camera does not suffer from noisy signals but has low data rate, slow and memory intensive. Consider a case where the image acquisition and processing time is less than 30 ms, it turns out that the maximum measurable natural frequency is less than 33 Hz. Moreover, increasing the camera frame-rate would not resolve the issue as the image acquisition and processing time will eventually become the actual bottleneck.

As for the accelerometer, the camera data is used to correct the accelerometer's data errors at a delay. The phenomenon of phase hysteresis and time delay degrades the performance of the control system or even induces instability [11]. On the other hand, the accelerometer signal is used to mitigate the delayed visual data into current time.

III. Mathematical Modelling Of Mobile Flexible Link Manipulator

A mathematical model is derived for the MFLM. The MFLM as shown in Figure 1 has three wheels. The mobile base is a three-wheeled platform. The front wheel is the driver (driven by a DC geared motor) wheel that has a tire. There are two rear follower wheels or caster wheels, which are free rolling. Thus the traction/braking and lateral forces are negligible for the rear wheels.

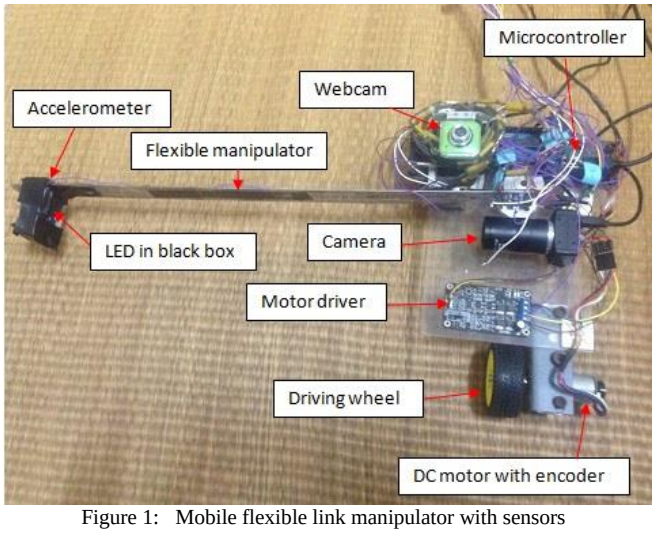

Figure 1: Mobile flexible link manipulator with sensors

A. Modelling the flexible manipulator

The flexible link manipulator considered in this research is a flexible beam with one end fixed to the base of the mobile platform, and a free end with a payload of M_p. We assumed that the flexible beam could only vibrate horizontally. Thus gravity effect can be neglected. Since the beam is long and slender, the length of the beam can be assumed to be constant and the deformation due to shear, the rotary inertia and the effects of axial forces are assumed negligible as well. Therefore, the Euler-Bernoulli beam theory (which applies to thin beam theory, where the rotary inertia and shear deformation are neglected) can be used to model the elastic behaviour of the beam. The displacement at the end point of the link from the fixed end is designated as $\delta(x, t)$. The governing equation of motion based on Euler-Bernoulli beam model is given by [12]

$$m\frac{\partial^2 w}{\partial t^2} + EI\frac{\partial^4 w}{\partial x^2} = f(x,t) \tag{1}$$

where w, m, E, and I are the transverse deflection, mass per unit length, Young modulus of elasticity, and second moment of area of the cross-section of the beam, and $f(x, t)$ is the loading per unit length of the beam. The general solution of equation (1) is [13]:

$$\begin{aligned}\delta(x,t) = {} & Ae^{-\zeta\omega_n t}\sin(\omega_d t + \phi).(\sigma(\sin(\beta x) \\ & - \sinh(\beta x) \\ & - (\cos(\beta x) + \cosh(\beta x))\end{aligned} \tag{2}$$

where:

$$A = \frac{\sqrt{(v_o + \zeta\omega_n y_o)^2 + (y_o\omega_d)^2}}{w_d^2}$$

$$\phi = tan^{-1}\left(\frac{y_o\omega_d}{v_o + \zeta\omega_n x_o}\right)$$

$$\omega_d = \omega_n\sqrt{1 - \zeta^2}$$

$$\omega_n = \sqrt{\frac{k}{m}}$$

$$\zeta = \frac{D}{2\sqrt{km}}$$

$$k = \frac{3EI}{L^3}$$

$$\sigma = -\frac{\sin(\beta L) + \sinh(\beta L)}{\cos(\beta L) + cosh(\beta L)}$$

where v_o, y_o, ω_n, ω_d, m, k, D, E and I are initial velocity, initial displacement, damped natural frequency, the mass of beam, beam stiffness and damping coefficient, Young's modulus and area moment of inertia of the beam, respectively. With L_l as the length of the beam, βL_l are the real roots of the equation:

$$\text{Cos}(\beta L_l)\text{Cosh}(\beta L_l) = -1$$

This transcendental equation has an infinite number of roots; the first 4 roots are given as βL_l = 1.87504, 4.694, 7.8547 and 10.9955, which can determine the natural frequencies of the beam as follows [13]:

$$\omega_n = \sqrt{\frac{EI}{\rho A}}\beta^2$$

For the beam used in this system, only first mode of vibration is noticed, yielding βL_l = 1.87504 and ω_n = 9.7474 rad/s.

To compute the beam vibration with varying payload at the tip, the effective mass of the beam needs to determined, where the distributed mass of the beam is represented by a discrete, end-mass. The effective mass m_e is:

$$m_e = 0.2235 m_b$$

where m_b is the mass of the beam. To include payload m_p at the tip of the beam, we compute total mass at the tip will be the effective mass m_e plus the payload m_p,

$$m = 0.2235 m_b + m_p \tag{3}$$

B. Modelling the mobile platform

The mobile platform is a three wheeled vehicle, with front wheel driven by a DC motor, and two rear free rolling follower wheels. For the mechanical characteristics, Newton's second law can be applied, yielding the equation:

$$\tau_m = K_i i = J_m \ddot{\theta}_m + \nu\dot{\theta} + \frac{\text{r}}{\eta} \tag{4}$$

where τ_m is the motor torque, K_i is the torque constant, i is the current, J_m is the moment of inertia for the motor, θ_m is the angular displacement of the motor, ν is the viscous friction, r is the coupling torque from the motor shaft to the wheel, η is the gear ratio. For the wheel, we have:

$$J_w \ddot{\theta}_w = \text{r} - R_w F_t - R_c F_w$$

where J_w is the moment of inertia for the wheel, θ_w is the angular displacement for the wheel, R_w is the radius of driving wheel, and R_c is the radius of rear wheels, F_t is the friction of driving wheel, and F_w is the friction of rear wheels. The electrical characteristic of the motor has the equation as:

$$V = \frac{di}{dt} + Ri + e = \frac{di}{dt} + Ri + K_e\dot{\theta}_m \tag{5}$$

Substituting equation (5) into equation (4), and performing mathematical manipulation, we get the transfer function as:

$$\frac{\ddot{\theta}(s)}{V(s)} = \left[\frac{K_i}{(J_m s+\nu)(R+s)+K_e K_i} \quad \frac{-(R+s)}{(J_m s+\nu)(R+s)+K_e K_i}\right] \tag{6}$$

where $\dot{\theta}$ is the angular velocity of the front wheel, V is the voltage input, L is the armature inductance, R is the armature resistance, e is the back-EMF of the motor, K_e is the back-EMF constant.

3.3. Model of mobile flexible link manipulator

Based on Lagrange's function formulation Λ, the dynamic equation matrix can be written as:

$$\begin{aligned}\mathcal{L} = {} & \frac{AL\rho\left(-8\dot{\delta}_o(v+\dot{\delta}_\text{o}) + \pi\left(2v^2 + 4v\dot{\delta}_\text{o} + 3{\dot{\delta}_\text{o}}^2\right)\right)}{4\pi} \\ & + \frac{1}{2}m_B v_B^2 + \frac{1}{2}I_B\omega_B^2 + \frac{1}{2}m_P\dot{\delta}^2 \\ & - \frac{1}{64}\pi^4\left[\frac{\text{EI}}{{L_l}^3}\right](\delta_o)^2\end{aligned} \tag{7}$$

where ρ is the density of the beam, m_B and v_B are the mass and velocity of the mobile base, I_B and ω_B are the inertia and angular velocity of mobile base. m_p is the mass of payload and δ_o is the initial beam deflection. E and I are Young modulus of elasticity and second moment of area of the cross-section of the beam. The flexible mobile manipulator dynamic equations obtained from the Euler-Lagrange's equations above can be re-written in matrix-vector form as follows:

$$M(q)\ddot{q} + R(q) = \tau \tag{8}$$

where $M(q)$ is the resultant forces matrix, $R(q)$ is the repulsive matrix, τ is the input torque matrix.

$$M(q) = \begin{bmatrix} AL\left(\frac{-16+6\pi}{4\pi}\right)\rho + m_P & 0 \\ 0 & m_B \end{bmatrix}$$

$$\ddot{q} = \begin{bmatrix} \ddot{\delta} \\ \dot{v} \end{bmatrix}$$

$$R(q) = \begin{bmatrix} \frac{EI\pi^4\delta_\text{o}}{32L^3} \\ 0 \end{bmatrix}$$

$$\tau = \begin{bmatrix} 0 \\ F_B \end{bmatrix}$$

The accelerations of the mobile base and deflection rate of the flexible beam can be obtained as:

$$\ddot{q} = M(q)^{-1}[\tau - R(q)] \tag{9}$$

The amount of deflection of the beam depends on the elasticity of the beam and the acceleration of the platform. Thus, we compute equation (9) for the base and the beam's deflection separately. The dynamic of the mobile base gives:

$$m_B \dot{v} = F_B$$
$$\dot{v} = \frac{F_B}{m_B}$$

The dynamic of the mobile flexible link manipulator gives:

$$\left\{ AL_l \left(\frac{-16 + 6\pi}{4\pi} \right) \rho + m_P \right\} \ddot{\delta} + \frac{EI\pi^4 \delta}{32{L_l}^3} = m\dot{v} \quad (10)$$

where $m = m_p + \rho AL_l$, that is mass of the payload and mass of the flexible beam. It is desirable to transform the dynamic equation (9) into state-space form. Defining the following state vector

$$X = [q^T \ \dot{q}^T]^T = [p \ \ \delta \ \ \dot{p} \ \ \dot{\delta}] \quad (11)$$

where p is the displacement of mobile base and δ is the deflection of the flexible link. We have the corresponding linear state-space model,

$$\dot{X} = \begin{bmatrix} 0_{2\times2} & I_{2\times2} \\ -M(q)^{-1}R(q) & 0 \end{bmatrix} X + \begin{bmatrix} 0_{2\times1} \\ M(q)^{-1} \end{bmatrix} \tau \quad (12)$$
$$Y = [I_{1\times2} \ 0_{1\times2}] \ X$$

IV. Sensors System Description

The manipulator is a flexible beam mounted on the mobile platform. The sensors are mounted on the MLFM as described in section 3. Table 1 depicts the parameter for the flexible beam.

Table 1
Flexible beam parameters

Parameter	Name	Value
Young's Modulus	E	190 GPa
Poisson's Ratio	ν	0.27 – 0.3
Area moment of Inertia	I	2.123×10^{-12} kgm^2
Cross-sectional area	A	0.96 x 28.8 mm^2
Length	L_l	53 cm
Density	ρ	7308.864 kg/m^3
Mass of beam	m_b	107.1 g
Stiffness	k	9.5376
Damping coefficient	D	0.024

The sensor system consists of: 1) accelerometer mounted at the back of the black box; 2) camera to capture the LED image inside the black box; 3) webcam for capturing the marking on the ceiling; 4) motor encoder. The accelerometer attached at the tip of the beam estimates the tip's vibration and the camera mounted at the fixed end of the beam captures the LED position at the tip, while webcam and encoder are used to estimate the velocity of the platform. The weight of the accelerometer is 14 g, while the LED with cardboard box has negligible mass. Applying equation (3), the total mass at the end of the beam m at no payload is 0.03756 kg, which includes the weight of accelerometer, the weight of LED, box, the wire connecting to the accelerometer and LED, and one-third of the beam mass. To validate the measurements from the accelerometer and camera, a range sensor (not shown in the picture) positioned at the tip to measure the tip vibration. Both the signals from the accelerometer and range sensor are captured by the data acquisition modules (National Instruments, NI 9201, NI 9233 and NI cDAQ 9172 chassis).

The accelerometer is MMA7260Q triple-axis accelerometer having 11 kHz internal sampling rate. The camera is the Firefly series FMVU-03MTC-CS, having a frame rate of 57 – 60 fps (frame per second), that frames a single LED fixed 50 cm over the beam tip. Calibration results showed that it has 1 mm accuracy (an averaged scale factor of 1 pixel/mm) measuring at 50 cm distance from the LED. In order to achieve the aforementioned frame rate, the acquired image has been reduced from 640 × 480 to 430 × 64 pixels, corresponding to the arc that the LED describes on the image plane. Timestamp exchange is used to predict the delayed visual data from the camera. For image processing operation, the coordinates of the LED on the image plane are evaluated through a blob detection operation.

A high accuracy short range infrared range sensor (Sharp GP2Y0A21YK) was used to measure the horizontal displacements at the tip of the vibrating flexible manipulator, while a long-range infrared distance measuring sensor was used to measure the distance travelled by the mobile platform. This short range infrared sensor can measure range between 0 cm and 80 cm.

A. Data from the sensors

A static investigation was carried out to measure the vibration at the tip of the beam. Figure 2 depicts the displacement computed from the accelerometer, camera and direct measurement from the range sensor. It was observed that the accelerometer's signal had a significant drift and the error increased overtime rapidly. This is due to the accumulation of error caused by double integration of the biased acceleration signal. The camera, on the other hand, was delayed with low data rate. The exposure time is set to the reciprocal value of the frame-rate. The camera operates a frame-rate of around 60 fps. Hence the exposure time is about 16 ms. A further delay is due to image processing.

For the experiment performed, information for the input signals has been obtained as follows:

- The accelerometer data acquisition sampled at 11 KHz. The acceleration data is double integrated into displacement estimates.
- Total time which includes an image capturing and processing the image is 96.8 ms for each coordinate of the LED on the image plane. The obtained value is then held until the next image is acquired.

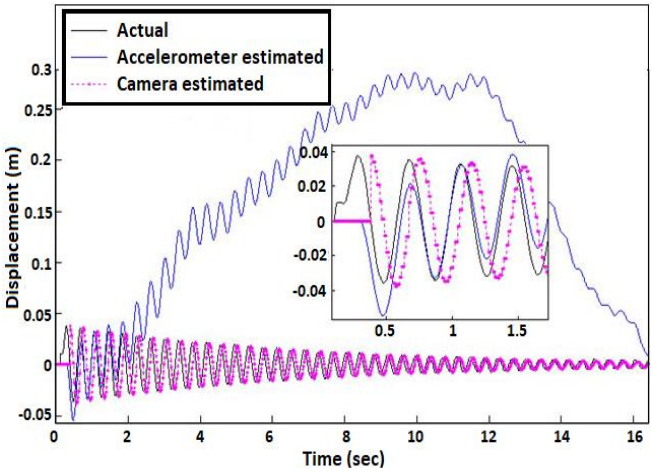

Figure 2: Comparisons of displacement estimation from accelerometer and camera (The actual displacement was measured from a range sensor)

An Extended Kalman filter is proposed to fuse the accelerometer and camera data. The algorithm works such that the drifted displacement estimates from the accelerometer is readjusted by the camera data through Extended Kalman filtering.

V. THE PROPOSED EXTENDED KALMAN FILTER

Dubus [14] used sinusoidal regression, which assumes the vibration is sinusoidal in shape, to reconstruct the vibration. In this paper, the model for the flexible beam system is used to reconstruct the vibration, while Extended Kalman filter for the nonlinear system has been applied to improve the estimation accuracy. This improves the estimation of the tip oscillation.

Figure 3 is the block diagram for the proposed algorithm. The algorithm works such that the modelled vibration waveform of the beam's response can be computed, and feed to the Extended Kalman filter as input *u*.

During the absence of camera data, the sensor update to Extended Kalman filter is based on accelerometer data. When the camera data is available, cross-correlation is first used to compute the delayed frame and the resulting visual data being readjusted and fed to the Extended Kalman filter's sensor update.

Consider the end-point displacement of the flexible beam which is tracked by *N* sensors. For simplicity, assume that the sensors' are having identical sampling rates; the signal model can be written as the state equation of the following form [15]:

$$x_{k+1} = f(x_k, u_k, n_k) \tag{13}$$

where, *k* is the discrete-time index, $x(k)$ is the state vector, $f(\cdot)$ is the generic non-linear functions relating the past state and current input, and n_k is the white Gaussian system noise of assumed known covariance matrix $Q_k = E[n_k n_k^T]$.

The measurements corresponding to the sensor is [15]:

$$z_{ik} = h_i(x_k, b_{ik}), i = 1 \dots N \tag{14}$$

with z_i the measurement vector of the sensor *i*, b_i the white Gaussian observation noise for the sensor *i* with zero mean and with assumed known covariance matrix $R_{ik} = E[b_{ik} b_{ik}^T]$, h_i is the measurement function associated with the sensor *i* and *N* is the number of sensors. Let $F(k)$ and $H(k)$ be the Jacobian matries of $f(\cdot)$ and $h(\cdot)$, denoted by $F(k) = \nabla f_k | \hat{x}(k|k)$ and $H(k+1) = \nabla h | \hat{x}(k|k)$. With the model described by equations (13) and (14), the multisensory Extended Kalman filter (EKF) can be computed as:

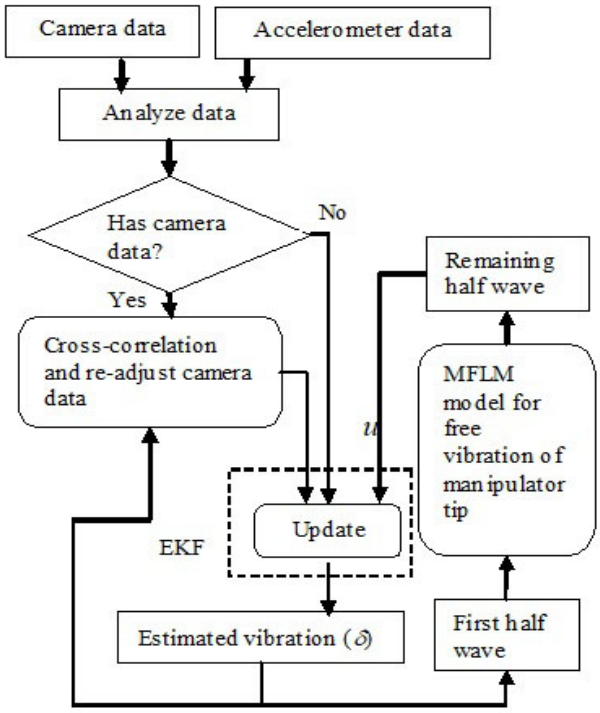

Figure 3: Block diagram of displacement estimation algorithm for flexible beam of Extended Kalman filter

- The estimation stage

$$\hat{x}(k+1|k+1) = \hat{x}(k+1|k) + \sum_{i=1}^{N} K_i(k+1)\left[z_{i(k+1)} - h_{i(k+1)}\hat{x}(k+1|k)\right] \tag{15}$$

$$K_i(k+1) = P(k+1|k)H_i^T(k+1)[H(k+1)P(k+1|k)H^T(k+1) + R(k+1)]^{-1} \tag{16}$$

$$P(k+1|k+1) = [I - K(k+1)\sum_{i=1}^{N} H_i^T(k+1)]P(k\_1|k) \tag{17}$$

- The prediction stage

$$\hat{x}(k+1|k) = f_k\hat{x}(k|k) + \mathrm{Bu(k|k)} \tag{18}$$

$$P(k+1|k) = F(k)P(k|k)F^T + Q(k) \tag{19}$$

where the *P* matrix provides the uncertainty on the estimate and *K* is the Kalman gain for the data fusion associated to the sensor *i*, and *u* is the control input. The innovation associated to the observation for the sensor *i* is given by $[z_i(k) - H_i\hat{x}(k|k-1)] = v_i(k)$.

A. *Determine optimum data fusion*

When both camera and accelerometer signals are available, Extended Kalman filter takes the fusion of both sensor data for estimation. When the camera data is not available, the Extended Kalman filter can take either 1) only accelerometer data; 2) combines accelerometer data with

previous camera data or; 3) combines accelerometer data with extrapolation of previous camera data. To determine the optimum data fusion during the absence of camera data, different methods of EKF algorithms were compared. For each set of inputs, the accelerometer data were tested with: i) original accelerometer data and, ii) accelerometer data re-computed at every windowed frame of previous accelerometer data of two cycles of vibrations.

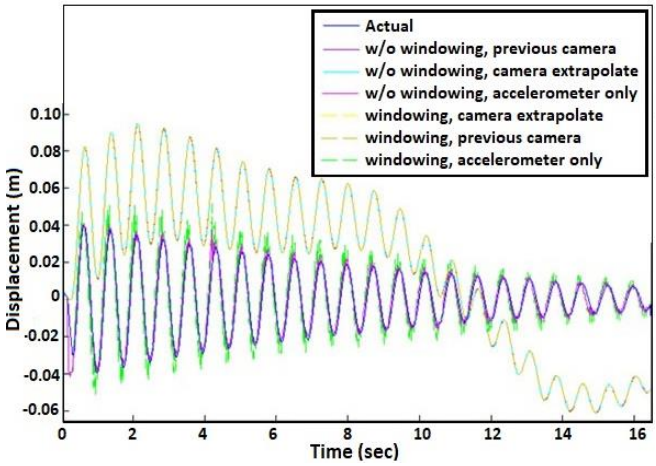

Figure 4: Comparison of sensor fusion methods using standard Extended Kalman filter

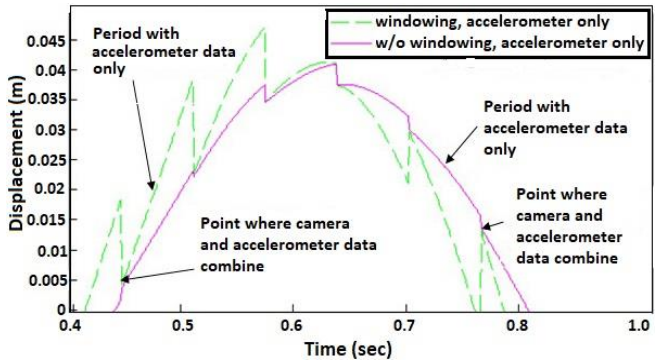

Figure 5: Illustration of case (1) EKF output

The experiments, with the setup as in Figure 1 were initiated by manually exciting the beam at the tip, and allowing it to vibrate freely. Figure 4 depicts the outputs for the design using the standard Extended Kalman filter. In case (1) (accelerometer only), there is no drifting but the outputs are showing rippling. This is due to during the absent of the camera data the EKF only compute the output using the accelerometer's signal. Once the successive data from camera arrives, the EKF computes the next output using the fusion of the camera's and accelerometer's data, thus resulting in the rippling output. Figure 5 illustrates the phenomenon.

On the other hand, for outputs that make use of previous camera data or extrapolation of previous camera data [case (2) and (3)], the output signals are smooth but showing output drifts. Here, the camera data is either using the previous or the extrapolation of previous camera data to fuse with the accelerometer's data. Thus, both the camera and the accelerometer data are always fused to produce the EKF output. Consequently, the output drifts could be due to the effect of the acceleration drift. Figure 6 illustrates the phenomenon.

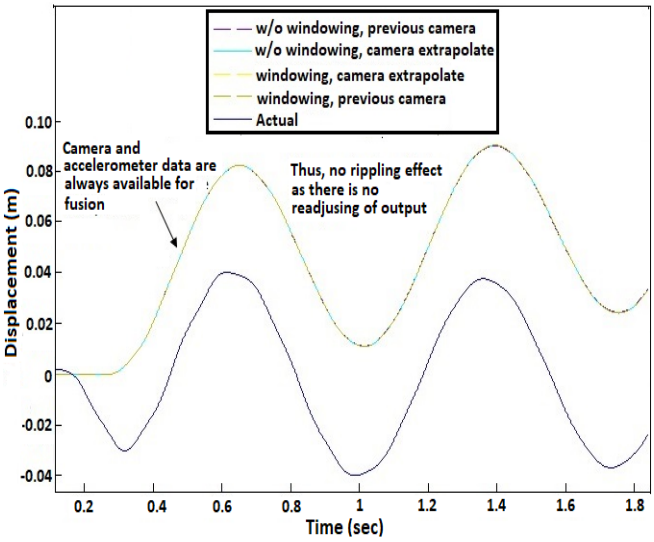

Figure 6: Illustration of case (2) and case (3) EKF output

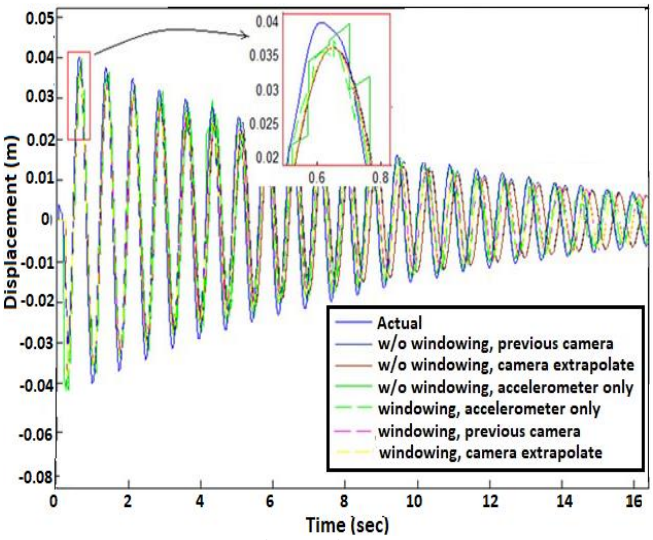

Figure 7: Comparison of sensor fusion methods using model-based Extended Kalman filter

Figure 7 depicts the outputs for the model-based Extended Kalman filter. There is no drifting for all outputs, while case (1) output for both with and without windowing of accelerometer data showing rippling of the signals (which is due to the adjustment of the signal when camera data presents). The rest of the outputs are smooth, with windowing previous accelerometer data and extrapolation of previous camera data showing a best match to the actual displacement.

It is therefore confirmed that the model-based Extended Kalman filter sensor fusion algorithm for vibration estimation gives accurate and smooth outputs in estimating vibration of the flexible beam.

B. Vibration prediction algorithm

Predictive controllers were developed in many research studies. Examples are model-predictive control (MPC) and finite element (FE) MPC. However, the literature on MPCs as effective vibration reduction strategy on flexible systems is very limited [16]. Abdolvand and Fatehi [8] presented a model-based prediction for vibration suppression of a flexible manipulator. Dubay et al. [17] utilized finite element based prediction to evaluate the behaviour of a flexible beam. The MPC based methods may lead to unsatisfactory performance when an accurate model is

unavailable, due to parameters uncertainty or truncation of high order vibration modes. Bakhti [18] developed an Extended Kalman filter observer to synthesize using the linear model of the flexible beam to predict the response of a beam. However, it provides a first-order approximation to optimize non-linear parameter estimation, which may include large errors. It often results in a surge of errors due to change in states. Ghahramani and Towhidkhah [10] proposed a generalised incremental predictive algorithm for predicting the vibration of a flexible joint robot. Shuai [19] proposed predictive control technique for the flexible manipulator. Wei and Liu [3] made use of the previous feedback trajectory and the feedback lag to calculate the corrected reference trajectory for flexible link manipulators. Tran et al. [20] proposed a multi-step ahead prediction for forecasting the machine's operating conditions using regression trees and neuro-fussy systems. The disadvantage is that they are based on linearization which it may not response fast enough to sudden change in state, inducing error.

In this paper, the state-space model is used to predict the future state using the present and previous states. The future state is then updated to the model to generate input to the EKF for prediction output multiple steps ahead. This approach combines the advantages of the model-predictive method and previous state feedback using present and previous states to the EKF, thus improves the trajectory prediction of the tip of the flexible manipulator.

Based on [10], both present and previous states are used for j number of steps ahead prediction. Based on the augmented state-space model, the future state variables are calculated sequentially using the set of future control parameters. For a one step ahead of state/output prediction, the linearized state-space model is [10]:

$$\begin{cases} x(k+1) = \Lambda x(k) + \text{B}u(k) \\ y(k+1) = \mathbb{C}x(k+1) \end{cases} \tag{20}$$

where $x \in \text{P}^n$, $u \in \text{P}$, and $y \in \text{P}$ denote the state vector, system input and system output, respectively. And, $\Lambda \in \text{P}^{n\times n}$, $B \in \text{P}^n$ and $\mathbb{C} \in \text{P}^n$ are system matrices. To predict the future response of the system, the change in the future control trajectory needs to be determined as:

$$\Delta u(k), \Delta u(k+1), \dots, \Delta u(k+N-1) \tag{21}$$

where N is the control horizon. The future state variables are denoted by

$$x(k+1), x(k+2), \dots, x(k+N) \tag{22}$$

The future state for one-state ahead prediction $k+1$ is:

$$x(k+1) = \Lambda x(k) + \text{B}\Delta u(k) \tag{23}$$

For two-states ahead prediction $k+2$, we can write the equation as:

$$\begin{aligned} x(k+2) &= \Lambda\, x(k+1) + \text{B}\, \Delta u(k+1) \\ &= \Lambda^2\, x(k)\, \Lambda\text{B}\Delta u(k) + \text{B}\Delta u(\text{k}+1) \end{aligned} \tag{24}$$

It follows that, the general form of j step-states ahead predictions can be formulated as:

$$x(k+j) = \Lambda^j x(k) + \sum_{n=1}^{j} \Lambda^{n-1}\text{B}\Delta u\,(k+j-n) \tag{25}$$

The outputs taken from vibration estimation approach developed in the previous section is then fed to $x(k)$, and the change in modelled output Δu of equation (25). The block diagram developed as shown Figure 3 is then modified to contain vibration prediction as shown in Figure 8.

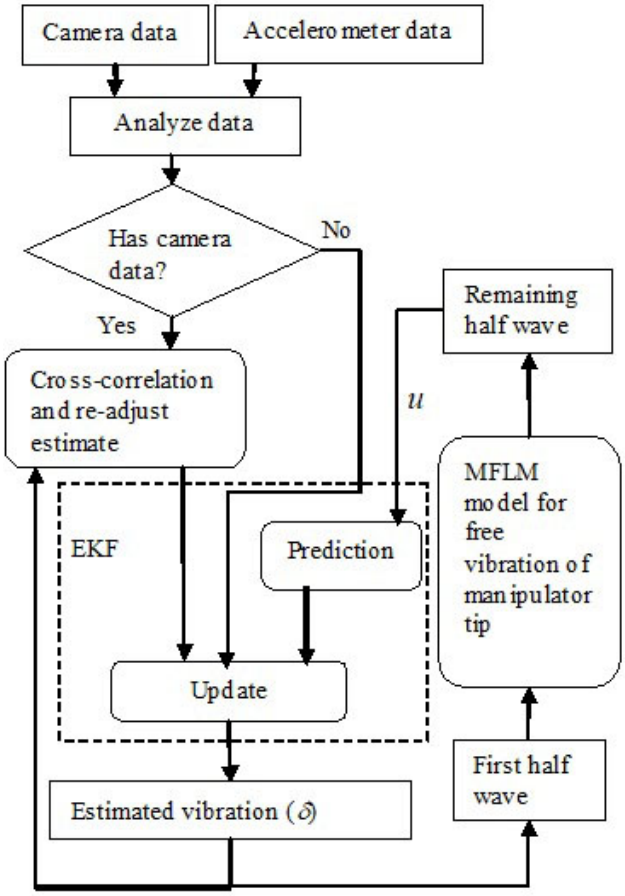

Figure 8: Block diagram of algorithm for vibration prediction for flexible beam

VI. Results And Discussions

Experimental verifications were carried out with 0.67V, 1.34V, 2.01V, 2.68V and 3.35V input to the driving motor of the platform, and with 10g, 30g, 50g and 70g load at the manipulator's tip for each input voltage, respectively. For the weight of 80g and above the platform begins to overturn, thus the experiments were carried out until 70g. Also, due to the space constraint of 2.4m of the experimental workspace, the experiment was run for 10 seconds straight path movement of the mobile platform.

The model based prediction algorithm (MP), EKF based prediction without modelled input (EKFP) and EKF based prediction with modelled input (EKFPM) were compared. 300 steps ahead prediction was set, leading to 150 milliseconds ahead prediction.

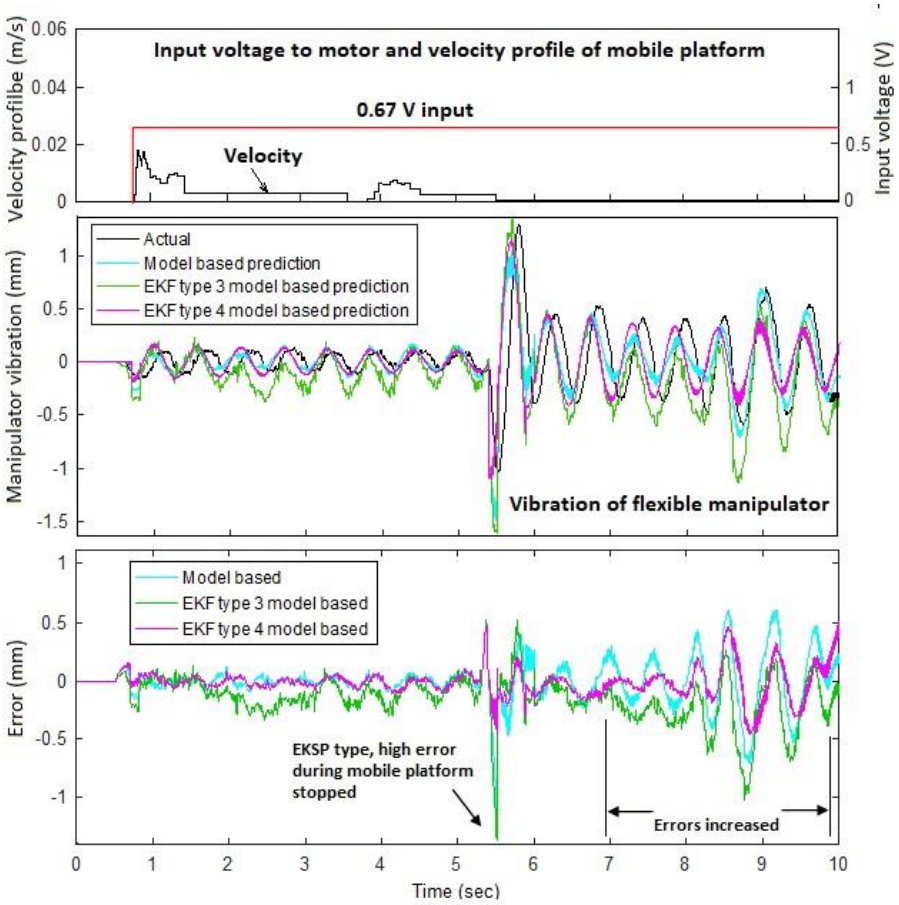

Figure 9: Comparison of prediction methods for 50g payload at the manipulator tip for 0.67V input

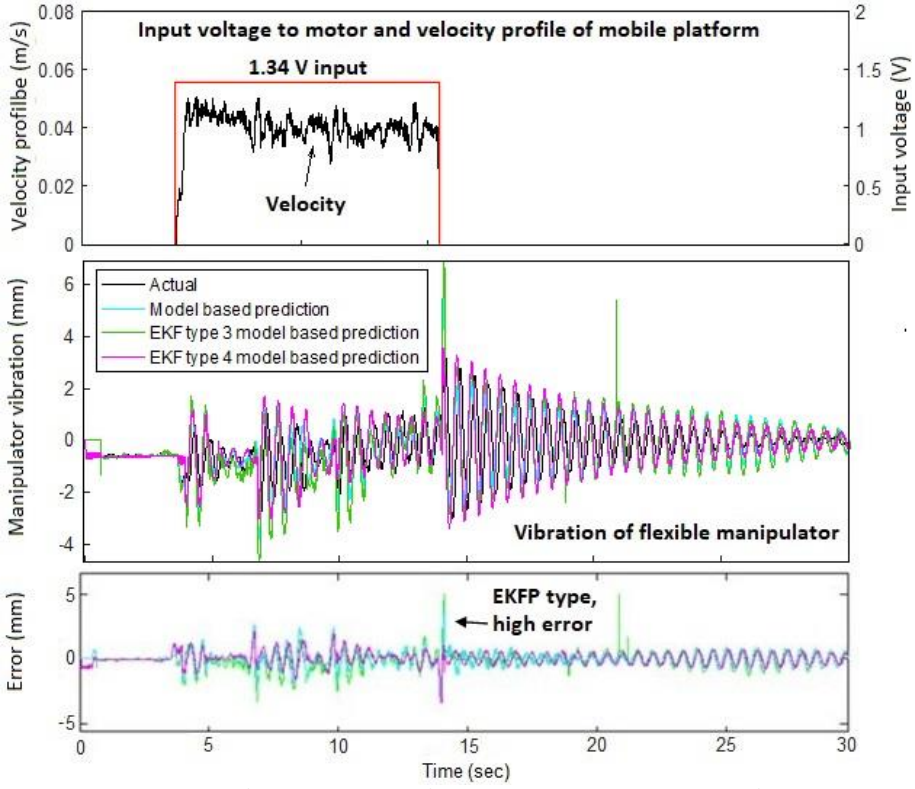

Figure 10: Comparison of prediction methods for 50g payload at the manipulator tip for 1.34V input

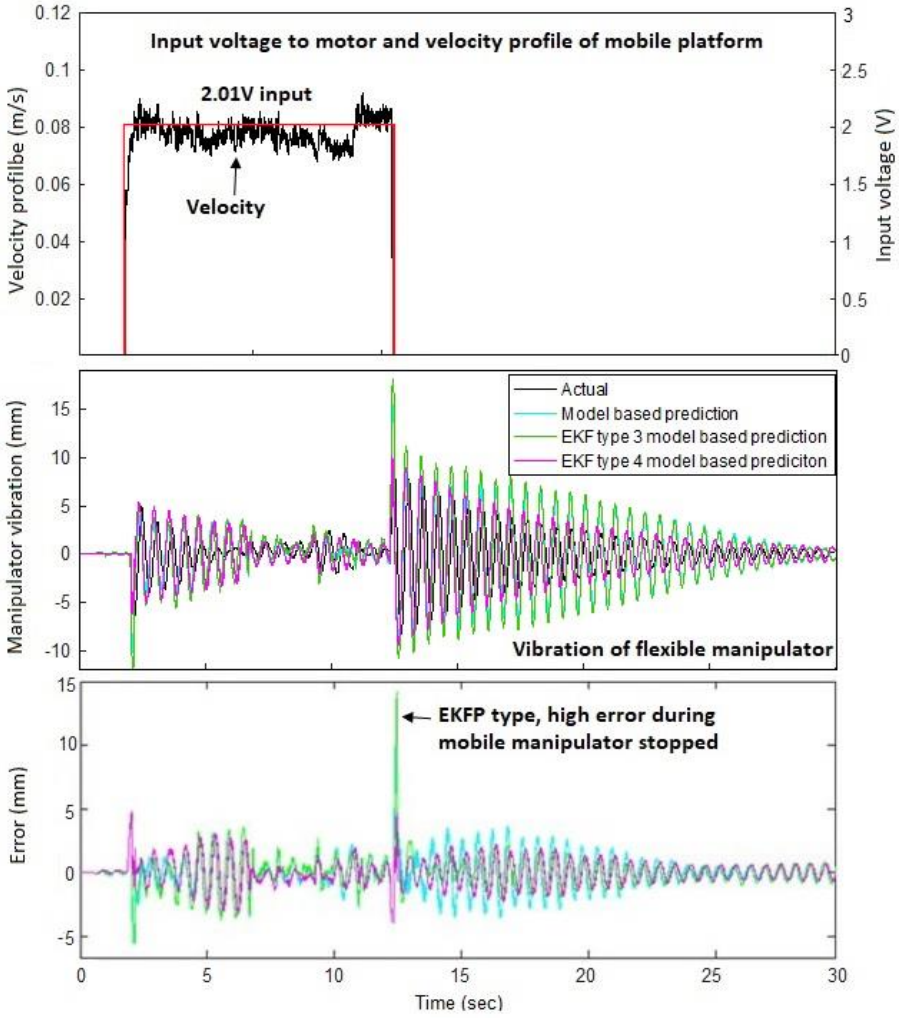

Figure 11: Comparison of prediction methods for 50g payload at the manipulator tip for 2.01V input.

Figure 9 to 11 above depicts the predicted transient responses of the flexible link manipulator with 50 g payload at the tip, at 0.67V, 1.34V and 2.10V inputs, respectively. It can be seen that there are spikes in the errors during when the platform starts and when the platform stops. The spikes in the errors are due to the sudden change in the vibration when the platform abruptly starts to move and abruptly stop.

It draws from the experimental results that the errors of the predictions are within 10 mm error for EKFP, and within 5 mm errors for MP and EKFPM. The results manifested that EKFP contributed to over prediction during a change input to the manipulator, thus resulted in overshoot in error at the input change. Comparing MP with EKFPM, the latter shows smooth and better match to the actual displacements. This showed that the EKFPM achieved the best prediction of vibration for the flexible manipulator for the MFLM.

Table 2 tabulates the RMSE and max error for the three types of model prediction methods for various payloads at the tip of the flexible manipulator, at various inputs. It can be seen that by increasing the speed of the platform there is an increase in the RMSE error for the three types of algorithms. There is no increase in errors for the increase in weight of payload at the tip of the manipulator.

Comparing the three types of methods, in terms of RMSE the EKFP has highest errors, while the EKFPM has lowest errors. As well, for the maximum error, the EKFP has very high errors as compared to MP and EKFPM. This proved that EKFPM is the best in terms of vibration prediction. This is due to the modelled input to the algorithm that helped to improve the accuracies.

Therefore, from the experimental results, the EKFPM is the best for use in predicting the future vibration for the manipulator for the MFLM. It is based on the modelled data in place of camera data and with modelled input to the EKF. The prediction errors are within 5 mm. EKFP that based on camera extrapolation and no modelled input to the EKF does not provide good vibration prediction of the manipulator of MFLM. It has the highest error of around 14 mm, as shown in Figure 11.

The experimental results achieved thus opened the way to a real-time implementation of the proposed technique for model predictive controllers having feedback lags.

VII. CONCLUSION

This paper presents a method to exploit the fusion of sensor measurements for predicting the vibration at the tip of a mobile flexible link manipulator. A model-based state predictive algorithm is incorporated to predict manipulator's reaction using the fusion of visual and inertial data. It is based on state prediction algorithm utilizing the model of the flexible beam on mobile platform as input. The technique here uses a model-based Extended Kalman filter to fuse the measurements from accelerometer and camera. The mathematical model finds the fit to shape of the beam oscillation and incorporated into the measurement data to

improve the accuracy and smoothness of the predicted output.

The effectiveness of the proposed vibration prediction system was examined. The experiments illustrated that algorithm can predict the vibration at the manipulator tip at varying payloads and varying input voltages to the driving wheel of the MFLM at a good accuracy.

Table 2
RMSE and maximum error for the three types of prediction methods

Predictive type		MP		EKFP		EKFPM	
Payload	Error / Speed	RMSE (mm)	Max error (mm)	RMSE (mm)	Max error (mm)	RMSE (mm)	Max error (mm)
No load	Speed 1	0.0011	0.79	0.0011	1.41	0.0008	0.55
	Speed 2	0.0036	4.2	0.0033	5.08	0.0028	3.83
	Speed 3	0.0013	4.89	0.0015	14.94	0.0012	4.96
	Speed 4	0.0039	5.08	0.0042	15.09	0.0035	5.17
	Speed 5	0.0052	5.37	0.0058	13.78	0.0046	5.05
10 g	Speed 1	0.0011	0.76	0.0011	1.4	0.0008	0.51
	Speed 2	0.0036	4.15	0.0033	5.07	0.0027	3.82
	Speed 3	0.0013	4.84	0.0015	14.94	0.0012	4.95
	Speed 4	0.0039	5.07	0.0042	15.05	0.0034	5.15
	Speed 5	0.0052	5.32	0.0058	13.75	0.0046	5.01
30g	Speed 1	0.001	0.71	0.001	1.37	0.0007	0.51
	Speed 2	0.0035	4.18	0.0032	5.02	0.0027	3.83
	Speed 3	0.0012	4.8	0.0014	14.88	0.0011	4.94
	Speed 4	0.0038	5.07	0.0041	15.01	0.0034	5.13
	Speed 5	0.0052	5.3	0.0057	13.72	0.0045	5
50 g	Speed 1	0.001	0.7	0.001	1.37	0.0007	0.5
	Speed 2	0.0035	4.1	0.0032	5	0.0027	3.8
	Speed 3	0.0012	4.8	0.0014	14.87	0.0011	4.9
	Speed 4	0.0038	5	0.0041	15	0.0034	5.1
	Speed 5	0.0051	5.3	0.0057	13.58	0.0045	5
70 g	Speed 1	0.001	0.67	0.0009	1.34	0.0007	0.47
	Speed 2	0.0034	4.08	0.0032	4.96	0.0026	3.77
	Speed 3	0.0011	4.72	0.0013	14.8	0.001	4.85
	Speed 4	0.0037	5	0.0041	14.98	0.0034	5.07
	Speed 5	0.005	5.3	0.0057	14.55	0.0044	4.98
Mean RMSE		0.00295		0.00311		0.0025	

The advantage of the proposed algorithm is its ability to provide a faster estimation speed. Therefore, it is useful for controller design with fast system dynamics. By yielding a better prediction of the manipulator responses, the proposed method enables better controller design schemes for vibration rejection or prevention.

The limitation is that the prediction does not predict external disturbances. Nevertheless, the camera attached at the base of the flexible beam provides a mean of allowing feature addition for feedback sensing capabilities. For instance, object recognition method can be motivated for future research in predicting the potential of disturbances.

REFERENCES

[1] S.K. Dwivedy and P. Eberhard, "Dynamic analysis of flexible manipulators, a literature review," *Mechanism and Machine Theory*. vol. 41, 2006, pp. 749–777.

[2] C.T. Kiang, A. Spowage and C.K. Yoong, "Review of Control and Sensor System of Flexible Manipulator," *Journal of Intelligent and Robotic Systems*. vol. 77, no. 1, 2015, pp. 187–213.

[3] X. Wei and S. Liu, "Computational Effective Predictive End-Point Trajectory Control of Flexible Manipulators with Measureable Feedback Lag," *Research Journal of Applied Sciences, Engineering and Technology*, vol. 4, no. 20, 2012, pp. 3875-3884.

[4] L. Bascetta and P. Rocco, "End-point vibration sensing of planar flexible manipulators through visual servoing," *Mechatronics*, vol. 16, no. 3-4, 2006, pp. 221–232.

[5] G. Dubus, "On-line estimation of time varying capture delay for vision-based vibration control of flexible manipulators deployed in hostile environments," *Intelligent Robots and Systems (IROS), IEEE/RSJ International Conference*, Taipei, Taiwan, 2010 Oct 18-22

[6] K. Uren and G. Van Schoor, "Predictive PID control of non-minimum phase systems," *Advances in PID control*, InTech, 2011.

[7] G.B. Avanzini, A.M. Zanchettin, and P. Rocco, "Reactive Constrained Model Predictive Control for Redundant Mobile Manipulators," *Intelligent Autonomous Systems*. vol. 13, 2015, pp. 1301-1314.

[8] M. Abdolvand and M.H. Fatehi, "Model-base Predictive Control for Vibration Suppression of a Flexible Manipulator," *UKACC International Conference on Control*, 2012 Sep 3-5, Cardiff, UK.

[9] G.G. Rigatos, "Model-based and model-free control of flexible-link robots: A comparison between representative methods," *Applied Mathematical Modelling*, vol. 33, 2009, pp. 3906–3925.

[10] N.O. Ghahramani and F. Towhidkhah, "Constrained incremental predictive controller design for a flexible joint robot," *ISA Transactions*, vol. 48, 2009, pp. 321 – 326.

[11] Z. Qiu, J. Han, X. Zhang, et al., "Active vibration control of a flexible beam using a non-collocated acceleration sensor and piezoelectric patch actuator," *Journal of Sound and Vibration*, vol. 326, 2009, pp. 438–455.

[12] P. Hagedorn and A. DasGupta, *Vibration and waves in continuous mechanical systems*. USA: Wiley; 2007.

[13] G. Genta, *Vibration dynamics and control*. Boston, USA: MA, Springer; 2009.

[14] G. Dubus, O. David, and Y. Measson, "A vision-based method for estimating vibrations of a flexible arm using on-line sinusoidal regression," *Robotics and Automation (ICRA), IEEE International Conference*; 2010 May 3-7; Anchorage, AK, USA.

[15] R. Havangi and M.A. Nekoui, "Teshnehlab M. Adaptive Neuro-Fuzzy Extended Kalman Filtering for Robot Localization," *IJCSI International Journal of Computer Science*, vol. 7, no.2, 2010, pp. 2.

[16] P. Boscariol, A. Gasparetto and V. Zanotto, "Active position and vibration control of a flexible links mechanism using model based predictive control," *J. Dyn. Sys., Meas., Control*, vol 132, issue 1, 2009, pp. 1-4.

[17] R. Dubay, M. Hassan, C. Li, and M. Charest, "Finite element based model predictive control for active vibration suppression of a one-link flexible manipulator," *ISA Transactions*, vol. 53, issue 5, 2014, pp. 1609-1619.

[18] M. Bakhti, "Active vibration control of a flexible manipulator using model predictive control and kalman optimal filtering," *International Journal of Engineering Science and Technology (IJEST)*, vol. 5, issue 1, 2013, pp. 165-177.

[19] X. Shuai, Y. Li, and T. Wu, "Real time predictive control algorithm for endpoint trajectory tracking of flexible manipulator," *J. Zhejiang U*, vol. 44, 2010, pp. 259-264.

[20] V.T Tran, B.S. Yang and A.C.C. Tan, "Multi-step ahead direct prediction for the machine condition prognosis using regression trees and neuro-fuzzy systems," *Expert Systems with Applications*, vol. 36, issue 5, 2009, pp. 9378–9387.